Universidade Estadual de Campinas

Unicamp E-Racing - FSAE Electric

Installation and Sizing of the CubeMars AK10-9 KV60 Actuator for an FSAE Autonomous Vehicle

Campinas, Brazil - December 2025

Introduction

In this report, we evaluate the selection process and the mechanical and electrical sizing of Cubemars' AK10-9 KV60 steering actuator. The installation approach prioritizes minimizing interference with the existing driver-operated vehicle due to the team's financial constraints that do not allow for a dedicated driverless-only platform. Furthermore, compliance with rules of the conventional (driver) category and the ergonomics of the human driver must be maintained, both of which introduce technical limitations on how the motor can be mounted to the vehicle.

Therefore, this report provides guidelines applicable both to teams operating dedicated driverless vehicle and to those working with a single car shared between driverless and driver categories.

Actuator Selection

Mechanical Design Considerations

In the mechanical design of the actuator, several criteria were evaluated, including physical dimensions, peak and continuous torque, precision, and operating speed. Regarding overall size, the most compact option was prioritized, as a smaller motor would simplify installation and reduce interference with the driver. In terms of torque, a peak value of approximately 23 N·m was targeted, although the actuator is expected to operate under lower loads during typical conditions. Finally, for positioning accuracy, a precision on the order of 0.5° was established as the design objective.

In this context, the AK10-9 KV60 emerged as the ideal choice. Despite its high output torque — 48 N·m peak and 18 N·m continuous, both more than sufficient for the intended application — the actuator remains remarkably compact. Its torque capability eliminates the need for an external reduction stage, which would not only increase the overall dimensions of the assembly but also introduce additional mechanical complexity during installation. Instead, the AK10-9 integrates the motor, transmission elements and sensing hardware into a single housing, resulting in a lighter and shorter unit compared to conventional motor-plus-gearbox arrangements. This compact, integrated architecture

significantly simplifies the mechanical layout and reduces intrusion into the surrounding structure.

As shown in the following image, *Figure 01,* the unit achieves its compact form factor through a coaxial arrangement of motor and transmission components within a 61.7 mm axial envelope, while the integrated mounting interface enables direct fastening without additional adapter structures.

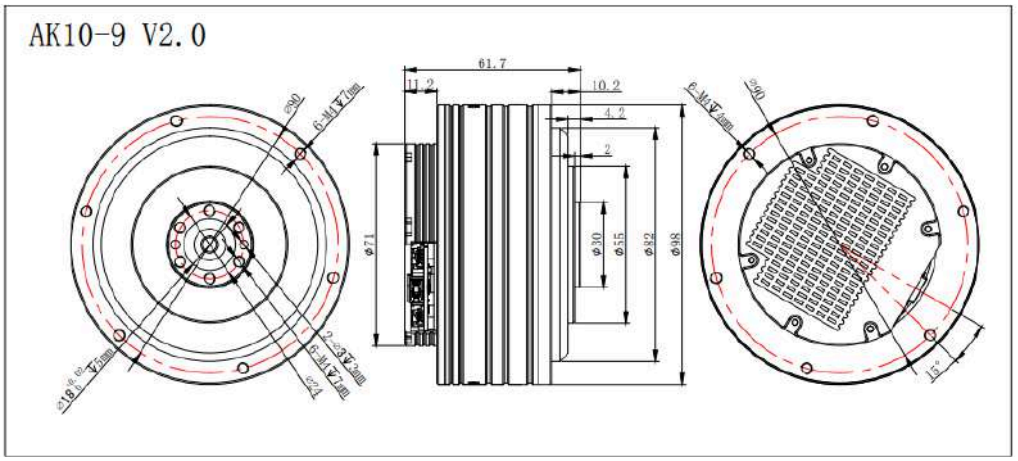

Figure 01: Technical drawing sourced from the CubeMars AK10-9 V2.0 KV60 product page.

Specification			
Insulation resistance	1000V 10MΩ	Phase to Phase inductance (μH)	181
Phase	3	Inertia (gcm²)	1002
Pole pairs	21	Km (Nm/√W)	0.45
Reduction ratio	9:1	Mechanical time constant (ms)	0.5
Back drive(Nm)	0.8	Electrical time constant (ms)	0.93
Backlash (°)	0.33	Weight (g)	960
Temperature sensor	NTC MF51B 103F3950	Maximum torque weight ratio (Nm/kg)	50
Noise dB 65CM away the motor	65	CAN connector	A1257WR-S-4P
Basic load ratings (dyn. C) N	2000	UART connector	A1257WR-S-3P
Basic load ratings (stat.C0) N	2520	Power connector	XT30PW-M
Rated voltage (V)	24/48	Inner loop encoder type	Magnetic encoder
Rated torque (Nm)	18	Inner ring encoder resolution	14bit
Rated speed (rpm)	109/228	Outer ring encoder type	Magnetic encoder
Rated current (ADC)	10.6	Outer ring encoder resolution	15bit
Number of encoder	2		

Figure 02: Motor specification table obtained from the official CubeMars AK10-9 V2.0 KV60 product page.

Another important criterion is steering speed. High-performance vehicles require fast steering response, and under our planned configuration operates at half of its maximum speed — approximately 110 rpm. At this speed, the lock-to-lock steering angle (208° plus an additional 7° of compliance, as permitted by FSAE rules) is achieved in about 307 ms, which is remarkably fast given the weight and mechanical resistance of the steering system.

In terms of precision, this actuator provides a 15-bit outer ring encoder resolution, as shown in the specifications in *Figure 02,* resulting in a theoretical angular precision of 0.011° (calculated as 360°/2^15). However, it is important to clarify that backlash is a mechanical clearance inherent to the gearbox design. When the motor shaft rotates through the 9:1 gear reduction, there exists a gap between the input gear and the gear connected to the output shaft. This clearance means there is space between the gears in the reduction stage where motion can occur without corresponding output movement.

The associated mechanical backlash is approximately 0.33° - also observed in *Figure 02*. While the encoder can theoretically resolve positions to 0.011°, the backlash of 0.33° represents the actual positioning limitation due to mechanical clearance in the planetary gearbox. This backlash remains well within acceptable limits for our application, as it does not interfere with the planned control trajectory. These characteristics confirm the suitability of the AK10-9 KV60 as the optimal solution.

Electrical Design Considerations

From an electrical perspective, we sought a high-performance motor that would not demand excessively high current, as this would directly impact battery sizing. We also prioritized a robust and reliable communication interface to ensure high levels of operational safety and system reliability.

It can be observed that at 23 N·m of torque the motor draws approximately 14 A, as indicated by the red curve in *Figure 03*. This makes it entirely feasible to operate using a

low-voltage battery pack without requiring a large number of parallel cells. Moreover, the motor typically operates near its highest-efficiency range (green curve in *Figure 03*).

It is also worth noting that the actuator can operate at either 24 V or 48 V. Using 24 V results in the maximum speed being reduced by half, which can be advantageous if the battery pack is not intended to be reconfigured with additional series cells. While operation at 24 V reduces maximum speed by half, torque output and overall efficiency remain unaffected within the nominal operating range. This allows the system to operate at 24 V and, when required, transition to 48 V to achieve higher performance in future iterations.

Regarding communication, the motor's CAN interface greatly simplifies integration. Connecting it directly to the vehicle's CAN network is sufficient for full control. Beyond its practicality, CAN is widely used not only in student formula cars but in the automotive industry as a whole. Its robustness provides a high level of reliability—an essential requirement for autonomous vehicle systems, particularly for safety-critical subsystems such as steering.

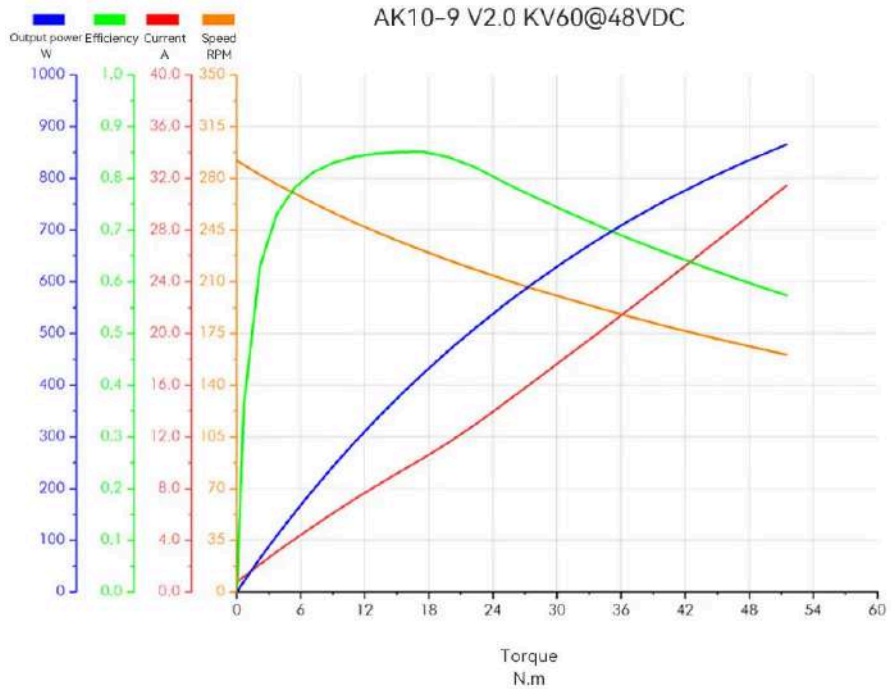

Figure 03: Graph of current, speed, efficiency, and power as a function of torque, obtained from the official CubeMars AK10-9 V2.0 KV60 product page.

Mounting and Integration

Mechanical

For the installation of the actuator in the vehicle, a perpendicular mounting plate was welded to the steering column, positioned above the driver's legs at the front hoop. This configuration keeps the actuator shaft aligned and parallel to the steering column, as in *Figure 04.*

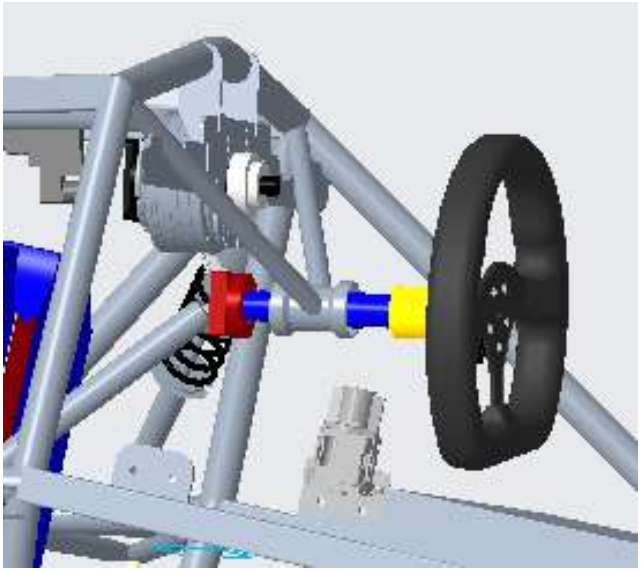

Figure 04: Pulley mechanism of the AK10-9 KV60 actuator, illustrated using the Creo CAD model

As illustrated in *Figure 04*, a small gap exists between the pulley attached to the steering column and the one mounted on the actuator shaft. These two 47mm pulleys are connected by a timing belt that transmits torque directly to the steering column. A key advantage of this belt-driven design is that the belt can be quickly removed to restore full manual steering control – ensuring compliance with FSAE regulations, which prohibit actuator-driven steering unless the mechanical steering system remains fully operational.

Furthermore, both pulleys share identical diameters, resulting in a 1:1 transmission ratio with no mechanical reduction between the actuator and the steering

column. The compact size of both pulleys ensures that driver ergonomics are not compromised, preventing any interference with the driver's ability to steer the vehicle.

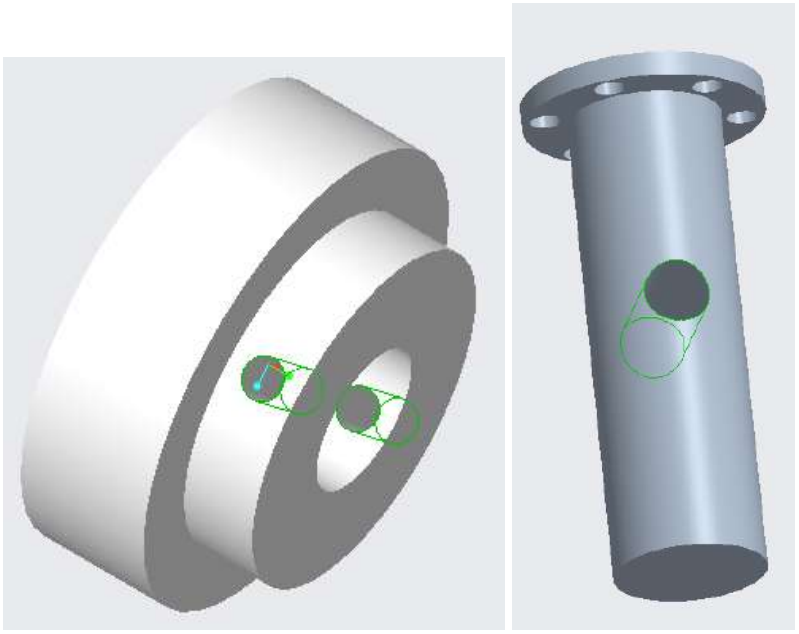

Figure 05 and 06: Actuator pulley CAD model created in Creo

The actuator pulley, detailed in Figure 05, features a radial through-hole that passes across its body. This hole accommodates a setscrew that locks the pulley to the actuator shaft, preventing both rotational slippage and axial displacement along the shaft.

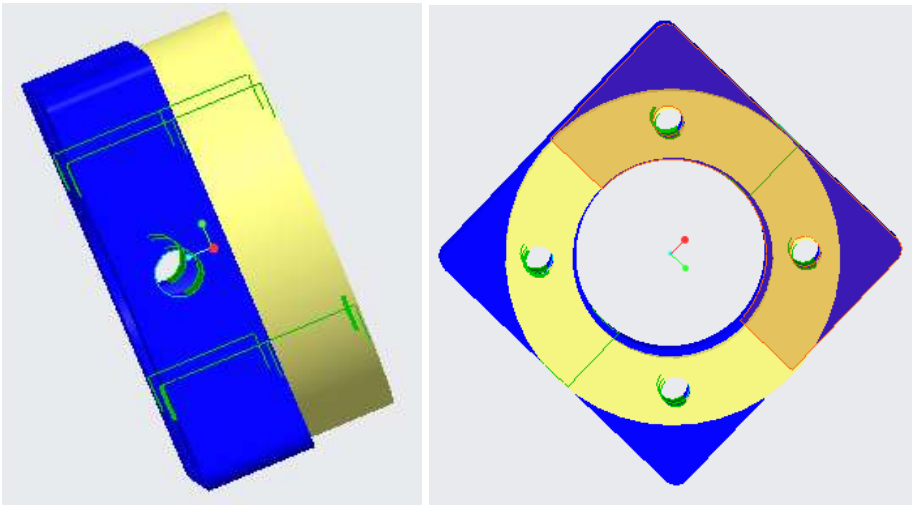

Figures 07 and 08: Steering column pulley and its mounting support, CAD models created in Creo.

Figures 07 and 08 show the steering column pulley assembly, which consists of two main components: a yellow pulley and a blue 3D-printed mounting bracket made of ABS (Acrylonitrile Butadiene Styrene). This bracket attaches directly to the steering column and is then bolted to the pulley using four screws, whose mounting holes are illustrated in *Figure 08*. This two-piece design eliminates the need to drill directly into the pulley teeth, preserving their structural

integrity. It is also important to note that the axial thickness of the bracket shown in *Figure 07* determines the pulley's longitudinal position on the steering column, allowing fine adjustments to ensure proper belt alignment with the actuator pulley during installation.

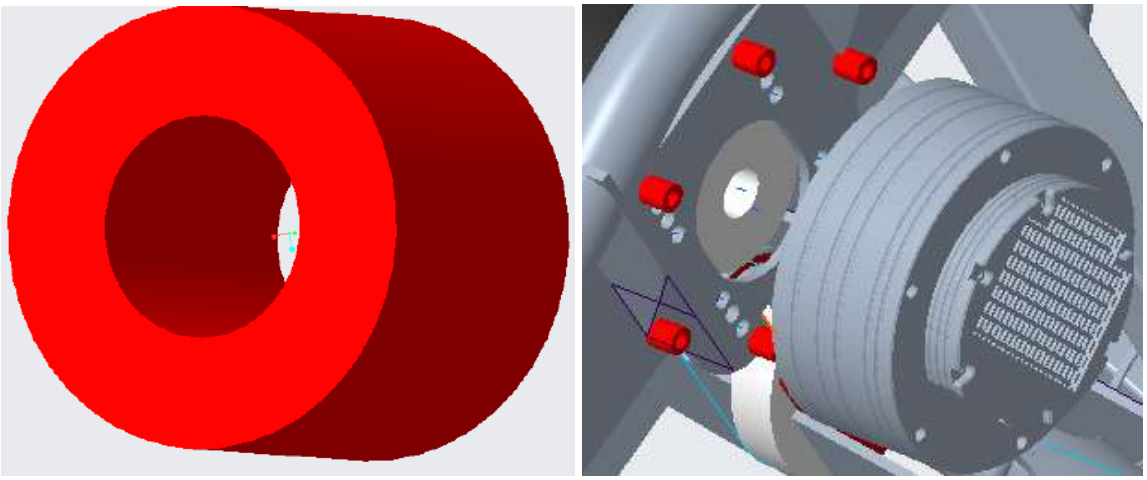

Figures 09 and 10: Actuator mounting assembly with spacers, CAD rendering created in Creo.

For the actuator installation, depicted in Figures 09 and 10, the existing mounting holes on the component were utilized. However, machining of spacers, such as the one in *Figure 09*, was required. These spacers provide the necessary offset from the mounting plate, ensuring that the actuator operates freely without any mechanical interference from the surface to which it is attached.

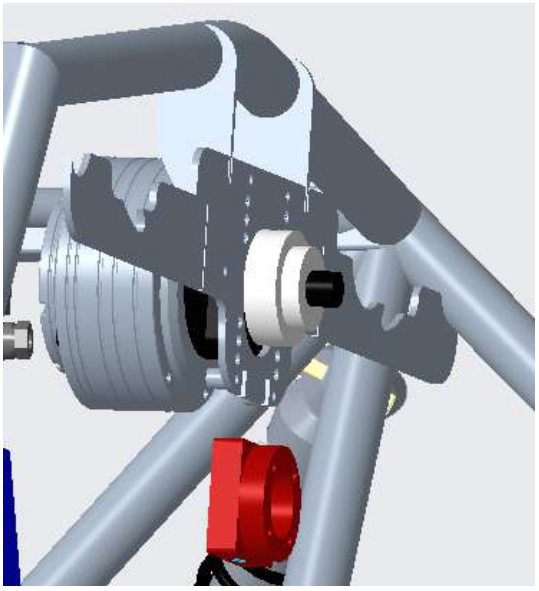

Figure 11: Creo model of the autonomous steering system with all components.

Figure 11 presents the complete autonomous steering assembly, integrating all mechanical components described above.

Electrical

In the electrical system, the motor was operated in servo mode. When combined with software-based calibration, this configuration enabled precise and smooth positioning. The calibration process was carried out using the *Rubik Link*, a device manufactured by Cubemars that not only performs motor calibration but also allows configuration of essential motor parameters. The R-Link (*Rubik Link)* acts as an interface between the actuator and the company's free configuration software, *CubemarsTool*.

Through this calibration, the actuator achieved high accuracy and smooth motion when reaching the desired position.

The communication protocol used was the actuator's native CAN interface, and the control messages were sent using the position–velocity mode, which allows transmitting position, velocity, and acceleration commands, as illustrated in *Figure 12.* These specifications were taken directly from the *AK Series Actuator Driver Manual.*

5.1.7Position and Velocity Loop Mode

Simplified block diagram of position velocity loop

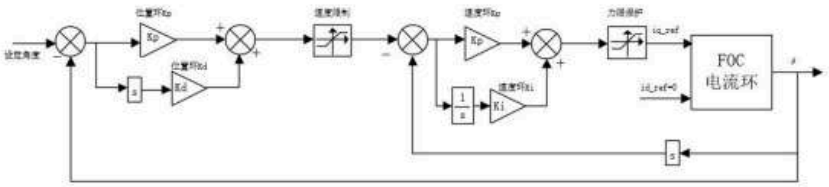

Position velocity loop mode sends data definition

Data bits	Data[0]	Data[1]	Data[2]	Data[3]	Data[4]	Data[5]	Data[6]	Data[7]
Range	0~0xff	0~0xff	0~0xff	0~0xff	0~0xff	0~0xff	0~0xff	0~0xff
Corresponding variables	Position 25-32 bit	Position 17-24 bit	Position 9-16 bit	Position 1-8 bit	Speed 8 bit high	Speed 8 bit low	Accelerated speed 8 bit high	Accelerated speed 8 bit low

Figure 12: CAN message structure for actuator control, extracted from the AK Series Actuator User Manual.

Another important aspect to highlight is the battery sizing. Since the AK10-9, like any motor, can experience current peaks, it is essential that the low-voltage battery is capable of delivering a sufficiently high peak current to meet the actuator's requirements. In this case, the vehicle already utilized cells capable of supplying discharge currents of approximately 60 A, which is more than adequate for the actuator, considering that *Figure 03* shows a maximum current draw of about 32 A. Even so, reaching this 32 A limit was not expected, as the vehicle's steering system requires a maximum torque of approximately 23 N·m at the steering column, which corresponds to approximately 14 A of current draw as shown in *Figure 03*.

Regarding energy autonomy, the autonomous category does not include an endurance event that demands high energy capacity. Therefore, an autonomy of 30–40 minutes is more than sufficient and is required only for testing purposes.

Practical Mechanical Installation

Figure 13 and 14: Front view of the actuator installation showing the belt drive connection and mounting plate configuration.

The mechanical installation phase revealed a few challenges that were not apparent during the CAD design stage.

Our first challenge was determining the optimal pulley diameter. Smaller pulleys minimize installation footprint and driver interference but increase belt stress and tooth skipping risk under load. After testing, we selected 47mm diameter pulleys as the best compromise between compactness and mechanical reliability, providing adequate tooth engagement while maintaining a low profile above the driver's legs, as seen on Figure 13.

With the pulley diameter established, the next challenge was finding a timing belt that properly connected both pulleys while maintaining correct tension. The belt needed to be short enough to maintain adequate tension without a tensioner mechanism, yet long enough to allow installation and removal for switching between autonomous and manual modes. We selected a SYNCHROBELT HT 48-3M-09 (72 teeth, 3mm pitch, 9mm width) with a 216mm pitch length.

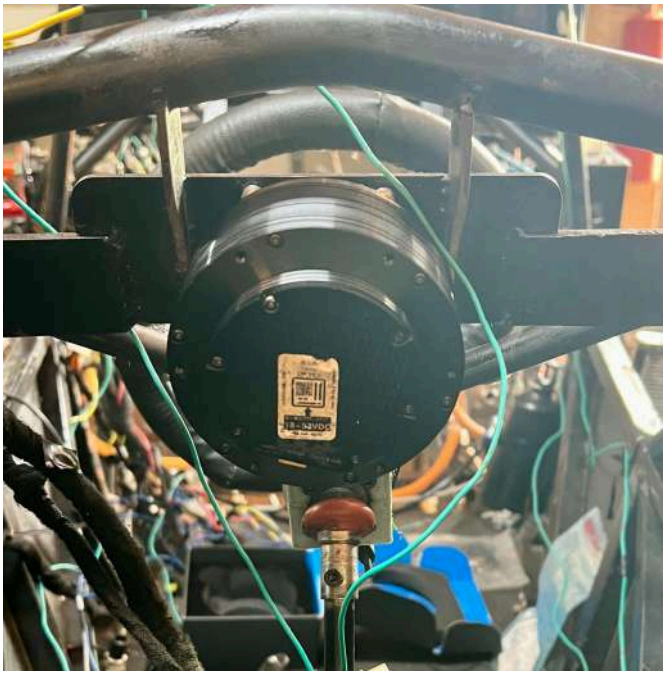

Figure 15: Back view of the actuator, parallel to the driving column

Once the belt drive system was defined, we proceeded to integrate it with the existing steering column. Drilling mounting holes in the steering column sleeve required precision to avoid weakening the structural integrity of this safety-critical component. The primary challenge was achieving the correct hole tolerances that would properly mate with the existing bracket without damaging it, which would have required manufacturing a replacement part. Finding the exact positioning and diameter that aligned perfectly with the bracket's geometry while maintaining adequate material thickness in the steering column proved critical to the assembly's success. The holes had to be accurately positioned to ensure proper pulley alignment while maintaining sufficient material thickness around the fasteners.

Finally, achieving parallel alignment between the actuator shaft and the steering column proved to be one of the most critical assembly challenges. Misalignment causes uneven belt loading, accelerated wear, and potential binding. Through iterative adjustment of the spacers shown in Figures 08 and 09, we determined that the actuator could tolerate up to 7° of angular misalignment before performance degradation occurred. Our final installation achieved a 2° misalignment, as observed in Figure 15,

which operates within acceptable parameters without compromising belt life or introducing unwanted friction.

Final Considerations

Finally, it can be observed that the AK10-9 actuator is highly suitable for Formula SAE autonomous vehicle projects. It offers an advanced control system that enables high positioning accuracy, while its compact construction allows for simple integration into steering systems, occupying minimal space within the vehicle. Additionally, its robust communication interface provides a high level of reliability, which is a critical requirement for high-performance Formula SAE vehicles that demand fast response times and dependable operation. The use of the CAN communication protocol—widely adopted in the automotive industry—further simplifies integration with the rest of the vehicle's control and software pipeline.

CubeMars Contacts:

https://www.cubemars.com/

https://www.linkedin.com/company/cubemars/

Unicamp E-Racing Author Contacts:

https://br.linkedin.com/company/unicamp-e-racing

thailon.oliveira@unicamperacing.com.br

helena.mandl@unicamperacing.com.br